PHYSICAL REVIEW C VOLUME 24, NUMBER 1 JULY 1981

Importance of nuclear viscosity and thermal conductivity and the analysis of the bounce-off effect in high energy heavy ion collisions

G. Buchwald, L. P. Csernai,* J. A. Maruhn, and W. Greiner
Institut für Theoretische Physik, Johann Wolfgang Goethe-Universität, Frankfurt am Main, West Germany

H. Stöcker
Gesellschaft für Schwerionenforschung, Darmstadt, West Germany
(Received 12 January 1981)

We present an analysis of high energy heavy ion collisions at intermediate impact parameters, using a two-dimensional fluid-dynamical model including shear and bulk viscosity, heat conduction, a realistic treatment of the nuclear binding, and an analysis of the final thermal emission of free nucleons. We find large collective momentum transfer to projectile and target residues (the highly inelastic bounce-off effect) and explosion of the hot compressed shock zones formed during the impact. As the calculated azimuthal dependence of energy spectra and angular distributions of emitted nucleons depends strongly on the coefficients of viscosity and thermal conductivity, future exclusive measurements may allow for an experimental determination of these transport coefficients. The importance of 4π measurements with full azimuthal information is pointed out.

[NUCLEAR REACTIONS $^{20}Ne + ^{238}U$, $E_{lab} = 400$ MeV/nucleon fluid dynamics, viscosity, heat conduction, cross sections.]

INTRODUCTION

Recent experimental data of the GSI-LBL-Marburg cooperation present evidence for 180° azimuthal correlations between fast, sidewards emitted light fragments and slow, heavy fragments in fast nuclear collisions (e.g., Ne+U, $E_{lab} = 400$ MeV).[1] This experimentally observed large collective momentum transfer has been interpreted in the nuclear fluid dynamical model as being due to the highly inelastic bounce-off effect[2] in collisions at intermediate impact parameters: Owing to the large pressure of the hot, dense matter in the impact region and its expansion, the projectile and target residues are pushed apart from each other in the scattering plane. This is in contradiction to the simple clear-cut fireball model,[3] separating the "fast" collision process from "slower" processes in the participant-spectator concept. Also, several other experiments[4-12] indicate strong transverse communication and a quasihydrodynamic behavior in fast nuclear collisions.

Since fluid dynamical calculations[2,4,13-22] predict that strong compression effects occur in fast nuclear collisions, such experiments are of great interest as they may offer a unique opportunity to investigate the properties of dense nuclear matter in the laboratory. We analyze for the first time the bounce-off process in a fluid dynamical model, including nuclear viscosity and heat conduction.[20] The important transport properties of nuclear matter, i.e., in our description the dissipative terms in the Navier-Stokes equations, have been included before only in one-dimensional calculations[15-18] and recently in an axially symmetric two-dimensional calculation,[19] which does not allow for the study of intermediate impact parameter reactions. Furthermore, we include a realistic treatment of the nuclear binding and the final thermal emission of free nucleons from the hot system.

Since these many physical effects are studied in our calculation, we had to drop, however, the three-dimensional treatment used before[2] because of numerical expenditure. But as the bounce-off effect proceeds in the scattering plane predominantly,[1,2] we expect reasonable validity for the two-dimensional calculation. We hope that we can handle the full three dimensional problem in the near future. Other models using different approximations have been applied to fast nuclear reactions and especially to the bounce-off process[23]; all seem to try to approximate a microscopic kinetic transport theory.

Models describing the hadron chemistry[24] and other kinetic models[23] consider the dynamics of the collision process, e.g., the geometrical aspects and the interactions between the nucleons, only poorly. In cascade calculations the nucleon-nucleon interactions are simplified and in some calculations even certain types of collisions are not considered. The hydrodynamical models assume chemical equilibrium and in the one-fluid case it is also assumed that locally the momentum distributions are close to the equilibrium

ones. In the discussed energy range these approximations are expected to be applicable[14-19] for the major part of the process. The Navier-Stokes equations also consider first order deviations from the equilibrium momentum distribution. The transport coefficients for the dissipative terms can be derived from kinetic theories[25,26] or deduced from experiments.[27]

The various hydrodynamical models seem to provide a rather realistic description of the process, especially in space and time. However, to describe the momentum space distribution and the fragmentation especially at the late stage of a reaction more realistically, an evaporation calculation has been attached to the hydrodynamical model.

THE FLUID DYNAMICAL MODEL

To analyze the bounce off effect in greater detail, we integrate the fluid-dynamical equations including shear (η) and bulk (ζ) viscosity, heat conductivity (κ), and a long-range nucleon-nucleon interaction in the form of a Yukawa potential:

$$\partial_t \rho + \partial_i(\rho v_i) = 0 , \tag{1}$$

$$\partial_t(\rho v_i) + \partial_j(\rho v_j v_i) = -\frac{1}{m}\partial_i p + \frac{1}{m}\partial_j[\eta(\partial_i v_j + \partial_j v_i - \tfrac{2}{3}\delta_{ij}\partial_k v_k) + \zeta\delta_{ij}\partial_k v_k] - \frac{\rho}{m}\partial_i u , \tag{2}$$

$$\partial_t(\rho E_T) + \partial_j(\rho E_T v_j) = \kappa\partial_j{}^2 T + \partial_i v_j\,[-p_T\delta_{ij} + \eta(\partial_i v_j + \partial_j v_i - \tfrac{2}{3}\delta_{ij}\partial_k v_k) + \zeta\delta_{ij}\partial_k v_k] , \tag{3}$$

where the indices i,j and k are running over the space coordinates and there is a summation for indices occurring twice in one term.

ρ is the nucleon number density, v_i is the ith component of the flow velocity, T is the temperature of the nuclear matter, and E_T is the thermal energy per nucleon. The total internal energy is separated into two terms:

$$E(\rho,T) = E_T(\rho,T) + E_C(\rho,0) , \tag{4}$$

$$E_T(\rho,T) = \tfrac{1}{2}\rho^{-2/3}T^2\left(\frac{4\pi}{6}\right)^{2/3}\frac{mc^2}{(\hbar c)^2} , \tag{5}$$

$$E_C(\rho,0) = \frac{K}{18\rho\rho_0}(\rho-\rho_0)^2 + W_0 , \tag{6}$$

where E_T is the total thermal energy resulting from the low T Fermi gas expansion. E_C resembles the short range nuclear interaction, i.e., the binding and compression energy, where K is the compression constant ($K = 200$ MeV), ρ_0 is the equilibrium nuclear number density ($\rho_0 = 0.17$ fm^{-3}), and W_0 is the binding energy at ρ_0 ($W_0 = -16$ MeV/nucleon.) Equation (6) is a parabolic fit to recent nuclear matter calculations and includes the kinetic energy of a free Fermi gas at zero temperature.[20] The pressure is calculated from the internal energy as

$$p = \rho^2\left.\frac{\partial E}{\partial\rho}\right|_{\sigma=\text{const}} , \tag{7}$$

and can again be separated into two parts, p_c and p_T, accordingly. To describe the long range n-n interaction a Yukawa potential is used which fulfills the equation

$$(\Delta - \alpha^2)U = -4\pi\beta\rho . \tag{8}$$

The parameters $\alpha = 2.1$ fm^{-1} and $\beta = -280$ MeV fm ensure the proper shape and surface properties of the nuclei in the ground state.

The temperature dependence[26,18] of the viscous terms in the Navier-Stokes equation is taken into account:

$$\eta = \frac{\sqrt{\pi m}}{8\sigma_{\text{tot}}}(T+T_0)^{1/2} , \tag{9}$$

$$\zeta = G\eta . \tag{10}$$

Here $\sigma_{\text{tot}} = 40$ mb and T_0 and G were varied in different calculations (T is given in MeV, $k_{\text{Boltzmann}} \equiv 1$). These viscosity values are in agreement both with fits to experiment[27] and theoretical considerations.[26] The viscosity coefficients however, are larger than those used by Tang and Wong.[19] Our viscous coefficients thus ensure a realistic shockfront thickness of 1.5–2.5 fm. The smaller values of the viscosity coefficients[19] may lead to numerical problems since the finite calculational mesh size causes a numerical viscosity.[28] We can roughly approximate the minimum value of the numerical viscosity by supposing that the shockfront thickness δ in the presence of the "numerical viscosity" will be approximately equal to the mesh size (as it was the case in Ref. 19. Using the approximations of Ref. 25 [Eq. (87.9)].

$$\delta = \frac{4}{\rho c_{\text{sound}}}(\tfrac{4}{3}\eta^* + \zeta^*) . \tag{11}$$

So the numerical viscosity ($\frac{4}{3}\eta^* + \zeta^*$) is of the order of 5 MeV fm$^{-2}c^{-1}$ in the case of a 0.5 fm mesh size in the discussed reactions.

The heat conductivity was fixed to the value $K = 0.015\ c/\text{fm}$.[19] Since the bounce-off process takes place in the scattering plane,[1,2] a detailed analysis of the characteristic dependence on η, ζ,

and κ may be done using a two dimensional Cartesian model.

THE EVAPORATION MODEL

At a late stage of the reaction the density becomes so small that the nucleons collide rarely. This stage lasts until the particles reach the detectors. During this stage the process cannot be described hydrodynamically because the conditions of small mean free path and thermal equilibrium are not fulfilled.[18,24] However, during this stage the particle density in momentum space remains constant in the absence of interactions.

In the previous "ideal fluid" calculations[2,14] the cross sections were calculated by taking into account the hydrodynamical flow velocities of the nucleons at a late stage of the process only. But even at these stages the nuclear fluid has a non-negligible temperature and the thermal velocities should be added to the hydrodynamical ones.[18,24,21] When the fluid reaches the breakup condition in our model the nucleons can explode into all directions due to their thermal and collective flow velocities.

The thermal momentum distribution of the nucleons inside a fluid cell i,j is described by the relativistic Fermi distribution:

$$f_{i,j}(\vec{p})d^3\vec{p}=\begin{cases}0\,, & \text{if } W_{ij}(p)<m\\ \dfrac{4}{(2\pi\hbar)^3}\dfrac{d^3\vec{p}}{\exp\{[W_{ij}(p)-\mu_{ij}]/T_{ij}\}+1}\,, & \text{for all other cases}\end{cases} \tag{12}$$

were $\mu_{i,j}$ is the chemical potential determined from the normalization condition at $\epsilon_{ij_{\text{bind}}}=0$, and $W(p)=(m^2+p^2)^{1/2}+\epsilon_{ij_{\text{bind}}}$. We take into account the binding properties of nuclear matter by shifting the distribution down in energy by the binding energy. Therefore only the high energy tails of the distribution are emitted as free nucleons. To obtain the momentum distribution of all nucleons in the laboratory frame the distributions[22] are Lorentz transformed to this frame by the relativistic boost velocity $\vec{\beta}_{i,j}$ of the cell i,j arising from the collective flow.[22,29]

$$f_{ij}^{\text{lab}}(\vec{P})d^3\vec{P}=\frac{w(\vec{P})}{W}f_{ij}[\vec{P}(\vec{P})]d^3\vec{P}\,. \tag{13}$$

Here $\binom{w}{\vec{P}}$ and $\binom{W}{\vec{P}}$ are the four-momenta in the cell and lab systems, respectively.

Thus from Eq. (13) we obtain the double differential cross section of the evaporated nucleons

$$\frac{d^2\sigma}{dW\,d\Omega}=\sum_{i,j}\frac{4V_{i,j}\sigma_0}{(2\pi\hbar)^3}\frac{A_{ij}(W^2-m^2)^{1/2}}{\exp[(A_{ij}-\mu_{ij})/T]+1}\frac{Z_T+Z_p}{A_T+A_p}\,, \tag{14}$$

where $V_{i,j}$ is the volume of the corresponding fluid cell, σ_0 is the geometrical cross section of the reaction, and

$$A_{ij}=\gamma_{ij}(W-\vec{\beta}_{ij}\vec{P}_{ij})\,. \tag{15}$$

In the above cross section the momentum vector $\vec{P}$ of the observed particle depends on the observation energy E and angles θ and ϕ:

$$\vec{p}=(W^2-m^2)^{1/2}\begin{pmatrix}\sin\theta\ \cos\phi\\ \sin\theta\ \sin\phi\\ \cos\theta\end{pmatrix},$$

where $W=m+E$. Up to now it was necessary to average the cross sections over the azimuthal angle ϕ and over different impact parameters to compare with experimental data. Since experimentally 4π-exclusive detectors are available and will be running soon, now these procedures are no longer necessary. Thus considerably more information can be gained about the collision process.

In contrast to the present model, earlier evaporation calculations did not take into account the binding and Fermi energy contained in the nuclear equation of state. These approximations therefore violated energy conservation during the transition from the interacting fluid phase to the free nucleon gas,[18,21] as well as the fluid-dynamical calculations without evaporation,[2,14,19] where the thermal energy was neglected. Thus all the previously obtained cross sections could approximate only the primary charged cross sections.[30] Figures 1(a) and 1(b) show the spectra for the Ne+U reaction at $E_{\text{lab}}=393$ MeV/nucleon and $b=4$ fm (b) with and (a) without binding. The difference is seen in the absolute value and in the shape of the spectra.

When binding is taken into account, only ~20% of the matter can escape as free nucleons, while the rest stays bound (i.e., in light or heavier nuclei). The exact portion of emitted free nucleons depends crucially on the viscosity and thermal conductivity coefficients used (see below). Furthermore, the spread in the energy and angular distributions is lower when energy conservation and binding are taken into account.

THE DYNAMICS OF THE BOUNCE-OFF PROCESS

The detailed analysis of the bounce-off effect was carried out in the reaction Ne+U at the pro-

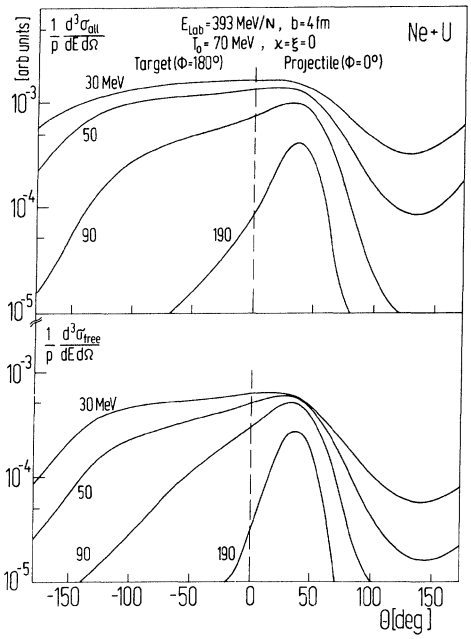

FIG. 1. (a) Invariant nucleon cross section of a Ne + U collision at $b = 4$ fm and $E_{1ab} = 393$ MeV/nucleon, shown separately in the projectile (right half) and target (left half) sides of the reaction plane. (No averaging over azimuth is performed.) Different curves belong to the indicated nucleon energies. Also the bound matter (see text) is considered. (b) Same as (a) but here only unbound, i.e., free nucleons are taken into account.

jectile energy $E_{1ab} = 393$ MeV/nucleon. In the two-dimensional Cartesian model both the target and the projectile are represented by cylinders of the same height, so that we obtain an approximately correct model of the flow process in the reaction plane. In the breakup moment the evaporation takes place in all directions. The transverse velocity component of the evaporated nucleons is produced by the thermal and Fermi motion, while in the reaction plane the collective flow velocities are still observable in the resulting cross sections. Since our aim is to analyze the effect of viscosity and heat conduction on the bounce-off process several calculations are performed for nonzero impact parameters and various transport coefficients η, ζ, and κ.

The reaction typically proceeds as follows: After the contact of the nuclei a shocked, hot dense zone develops. After half the reaction time ($t \approx 17$ fm/c) and at intermediate impact parameter ($b = 4$ fm) roughly half of the target nucleons are in the hot zone. The other target nucleons are still undisturbed because the shockfront propagates with supersonic shock velocity. The shocked nuclear matter behind the front remains compressed and heated for a while: $\tau \approx 30$ fm/c. The width of the shockfront separating the compressed and the undisturbed matter is about 1.5–2.5 fm depending on the transport coefficients. The maximum compression is around double nuclear density and the maximum temperature lies between 38 and 45 MeV depending on viscosity and heat conductivity. The heat energy ranges from 15 to 25 MeV/nucleon. (See Table I.) It has to be mentioned that these energy and temperature values do not contain the heat produced by the "numerical viscosity." It is approximated and considered separately in the calculation. The obtained temperature and density maxima are 10–30% lower than the values obtained from one-dimensional Rankine-Hugoniot shock calculations.[13,22] This is caused mainly by the additional coordinate in which the matter can be squeezed out in our calculation.

In the hydrodynamical expansion stage further heat is produced by the viscosity, and at the breakup time (35–40 fm/c) a non-negligible average temperature ($T = 10$–15 MeV) is observed. Thus, at the late stages of the collision process the observed heat energy is 2–3 times higher than the one given in Ref. 19.

The characteristic spatial form of the shocked zone is shown in Fig. 2. The compressed hot matter forms a curved zone of 2–3 fm diameter. Owing to high pressure in the shock zone the

TABLE I. Dependence of the maxium density ρ_{max}, maximum temperature T_{max}, produced heat, and evaporated unbound nucleons on the transport parameters η and κ. Heat produced by the numerical viscosity is not involved in the values listed here.

ρ_{max} ($1/\rho_0$)	T_{max} (MeV)	$\overline{E_{heat}}$ (MeV/nucleon)	$N_{nucleon}$	η_0 (MeV/fm^2c)	ξ_0	κ_0 (c/fm)
2.28	38.8	15.4	77.6	5.3	0	0
2.26	43.5	21.9	87.5	14.2	0	0
2.24	45.5	24.6	91.08	18.6	0	0
2.29	36.5	14.6	75.06	5.3	0	0.015
2.23	41.6	20.6	84.5	14.2	0	0.015
2.21	43.8	23.4	87.9	18.6	0	0.015

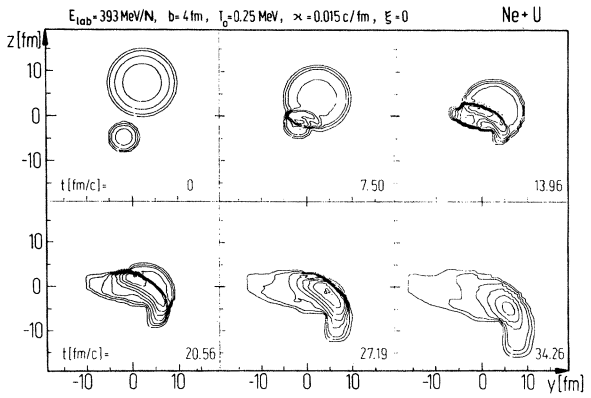

FIG. 2. Density contour plots of the Ne+U reaction at $E_{lab}=393$ MeV/nucleon and $b=4$ fm calculated in the equal speed system. The dynamical features can be seen in the sequence from $t=0$ to 34.26 fm/c. The zero temperature shear viscosity is $\eta_0=5.3$ MeV/fm^2c.

residual cold projectile and target fragments are pushed to the side. While the shockfront is propagating further into the target, the shock wave has already propagated through the projectile. The compressed mixture of projectile and target matter slides along the shockfront and expands to the upper hemisphere.

The heat produced by shear viscosity and the dissipation in the shockfront is first concentrated in the compressed matter. Later on, owing to heat conduction and to the propagation of the shock wave, however, the rest of the target and projectile are heated up also.

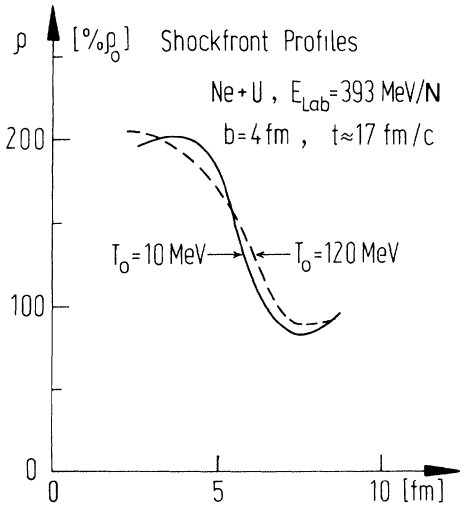

FIG. 3. Shockfront profile for two different viscosities. For $\eta_0=5.3$ MeV/fm^2 we are approximately in the region of numerical viscosity and the front thickness is about 1.5 fm. For $\eta_0=18.6$ MeV/fm^2c the front becomes considerably broadened.

THE INFLUENCE OF THE TRANSPORT COEFFICIENTS

The dependence of the dynamics on the transport coefficients can clearly be seen in Table I. Increasing the viscosity, i.e., the friction, both T_{max} and E_{heat} are enlarged too. The shockfront is broadened by viscosity (see Fig. 3) and additional thermal pressure is built up. A similar effect is caused by heat conduction. Here the heat is transported away from the shockfront which is broadened again. Owing to the smaller thermal pressure more matter is compressed. With increasing viscosity the influence of κ on T_{max}, E_{heat}, and shock thickness decreases. This may be understood as being due to the finite "transport capacity" of κ.

At the breakup time a part of the matter can be emitted as free nucleons. This evaporation is simulated by releasing only the nucleons which have positive energy after the binding energy is subtracted from the Fermi distribution, as described in Sec. III. Obviously the number of evaporated nucleons is different in the various regimes of the reaction and depends strongly on the breakup temperature and density: The rather cold target emits fewer free nucleons and they contribute mainly to the lower energy part of the spectrum, contrary to the nucleons stemming from the projectile and the shock zone. This can clearly be seen in the ϕ-dependent differential cross sections depicted in the reaction plane in Fig. 1(b). The target and projectile sides have strongly different characters. The nucleons evaporated from the target have a broad angular spread at low energies, corresponding to the deflection of the heavy target residue. The energy spectra of the target side fall down rapidly [Fig. 4(a)] at higher energies owing to low temperatures. Before we discuss the upper (projectile) hemisphere let us briefly reflect on the energy spectra at the target side [Fig. 4(a)] with viscosity. The yield at 120 MeV is already one order of magnitude below that at 10 MeV. From these slopes one could deduce a temperature of about 10 MeV assuming a Boltzmann distribution. However, we know that the actual temperature in the target residue is considerably lower. The shift to higher energies results from the collective sidewards motion of the target. This shows that it is dangerous to extract temperatures simply from the slope of the energy spectra.

On the projectile side the angular distribution is centered at $\theta_{def}\approx 40°$–$50°$ with a comparatively narrow angular spread [Fig. 1(b)] (20°–40°). Owing to the strong sidewards deflection of the projectile and the shocked matter, and the higher

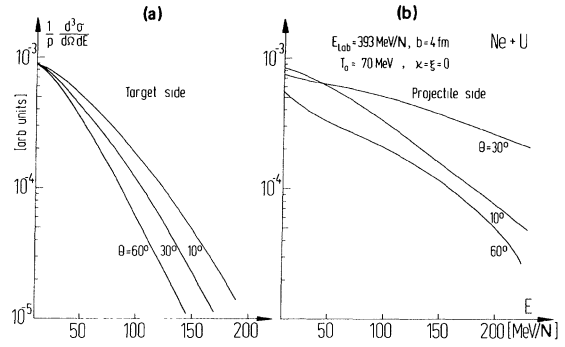

FIG. 4. (a) Free nucleon energy spectrum for Ne+U, $E_{1ab}=393$ MeV/nucleon, $b=4$ fm at the target side ($\phi=180°$). For three different angles in the reaction plane the curves behave similarly to each other. (b) Free nucleon energy spectrum of the same reaction but at the projectile side ($\phi=0°$). In the deflection direction of the projectile ($\Theta_{1ab}\approx 30°$) many fast and hot nucleons are observed. At other angles the high energy contribution is larger than in case (a).

temperatures on the upper hemisphere, the energy spectra at the deflection angle θ_{def} tend to much larger energies. On the projectile side we find a much larger yield at high energies. Especially at the deflection angle of the projectile side $\theta_{def}\approx 30°$, i.e., where we find the peak in the angular distribution, many fast particles are observed. Here, because of the smaller slope, a higher temperature than in the target [Fig. 4(b)] could be extracted. However, in analogy to the target case, we see that the energy spectra result from the thermal evaporation added to the collective sidewards flow of the matter, which dominates in this case. Therefore the "obvious temperature" extracted from the spectra exceeds by far the actual temperature of $T^{max}\approx 40$ MeV.

At forward angles the low energy target evaporation dominates. No highly energetic "leading fragments," i.e., forward moving projectile spectators, are observed in our calculations. This shows that for a given impact parameter (e.g., $b=4$ fm) the collective deflection is rather well defined, possibly allowing a determination of the impact parameter by measuring the deflection function in strongly correlated bounce-off events. Obviously, in inclusive experiments the angular spreads will be increased essentially because of the averaging over a range of impact parameters: For increasing impact parameter the deflection angles are shifted (see below).[2,20,23]

INFLUENCE OF THE SHEAR VISCOSITY

When the shear viscosity is increased, the collision process and the observables are altered considerably. To illustrate this quantitatively we discuss the angular distributions at 10, 90, and 190 MeV separately. We took the values for T_0 as 10, 70, and 120 MeV, corresponding to a η_0 at zero temperature of 5.3, 14.2, and 18.6 MeV/fm^2c, respectively. The dominant part of the low energy (10 MeV) particles stems from the target evaporation. As η_0 increases, the mean temperature rises. Thus the low energy part in the spectrum will become smaller, as can clearly be seen in Fig. 5(a). Especially the target heats up more, broadening and diminishing the flat maximum in the angular distribution in the lower hemisphere even more. In the angular distribution at $E_{kin}=90$ MeV, however, the target can be seen more clearly: When η is increased a shoulder is seen in the angular regime 30° to 130°. This results from the higher transverse momentum transfer to the target and from the high temperature in the target, both due to the increased viscosity. From $\eta_0=5.3$ to $\eta_0=18.6$ MeV/fm^2c this affects the cross section nearly by a factor of 2, and the peak on the projectile side is broadened. Only at high en-

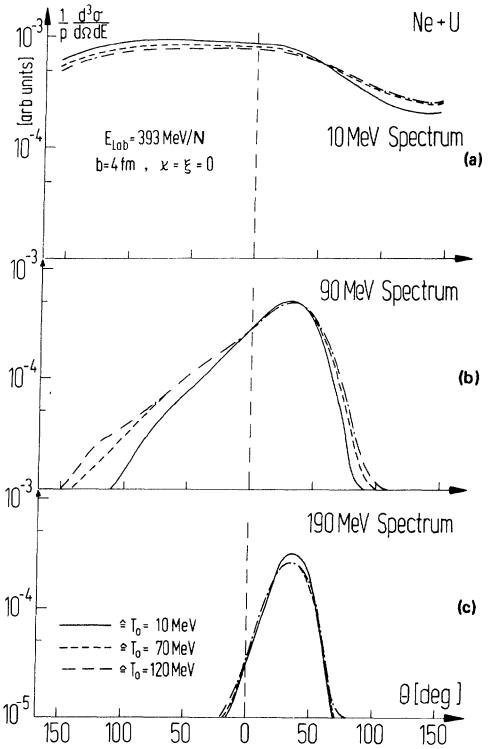

FIG. 5. Influence of the shear viscosity on the cross section. Invariant free nucleon cross sections for (a) 10 MeV, (b) 90 MeV, and (c) 190 MeV nucleon energy are shown separately in the reaction plane. The temperature dependent η was used [see Eq. (9)] with $T_0=10$ MeV (full lines), $T_0=70$ MeV (broken lines), and $T_0=120$ MeV (broken/dotted lines).

ergy [Fig. 5(b)] is it lowered by additional heating. But no drastic shift of the deflection angle (i.e., peak position) can be observed.

INFLUENCE OF THE HEAT CONDUCTION

The effects of heat conduction on the observables are somewhat smaller than expected due to Ref. 19. But for all viscosity values $\eta_0 = 5.3$ to $\eta_0 = 18.6$ MeV/fm^2c the influence of κ is similar. In Fig. 6 we consider, for example, the results for $\eta_0 = 18.6$ MeV/fm^2c.

The angular distribution for 10 MeV is nearly the same for $\kappa = 0$ and $\kappa = 0.015$ c/fm [Fig. 6(a)] but it is systematically a little higher for the heat conductive case. For the middle energy region, i.e., 90 MeV [Fig. 6(b)], the strongest influence of κ is observed. Here the tails for large angles are damped due to cooling of the corresponding particles. This can be seen in Table I where the maximum temperature as well as the maximum mean heat energy are smaller for $\kappa = 0.015$ c/fm, resulting in a smaller number of "unbound" nucleons. Clearly this cannot affect the cross-section part stemming mainly from collective kinetic effects as it is the case for high energies [Fig. 6(c), 190 MeV]. Here both cross sections are approximately the same.

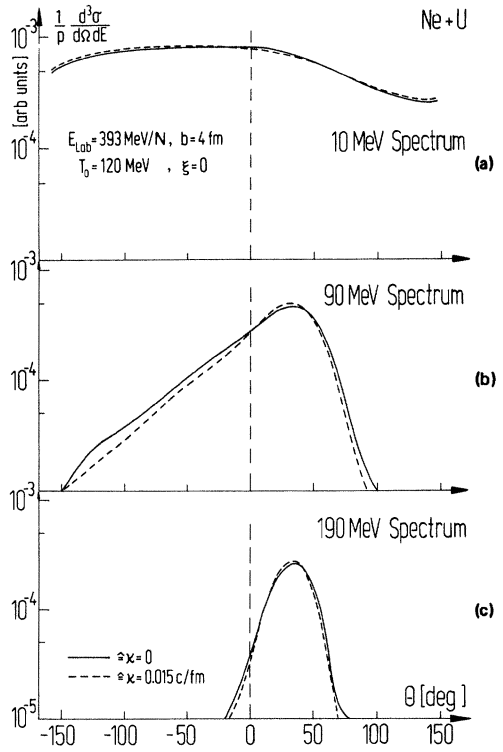

FIG. 6. Influence of the heat conductivity on the free nucleon cross section. The energy separation is the same as in Fig. 5. The full lines (broken lines) belong to heat conductivity of $\kappa = 0$ ($\kappa = 0.015$ c/fm).

DEPENDENCE ON THE IMPACT PARAMETER

Via the maxima on the projectile side of the spectra we can deduce a deflection angle of the projectile. This angle depends strongly on the impact parameter (Fig. 7).[20] Because the dependence is nearly linear over a wide range this would be a good tool for selecting distinguished impact parameters.

An interesting point is the dependence of the temperature on the impact parameter (Table II). Here two effects seem to overlap so that a maximum T may occur at $b = 4$ fm. The first effect which produces heat is the friction via the shear viscosity which is clearly most important at high b. The other effect is the heat production because of compression which dominates for low b. Here the heated zone is very large, whereas at high b the heated zone is smaller. Therefore the average heat energy increases monotonically with decreasing b. The cross sections for 190 MeV (Fig. 8) show impressively how the bounce-off effect dominates for large b and how its influence decreases for more central collisions. The difference in the 190 MeV cross section is about one order of magnitude for $b = 6$ and $b = 2$, respectively.

SUMMARY AND OUTLOOK

Summarizing the various results of our calculations the following conclusions can be drawn. In

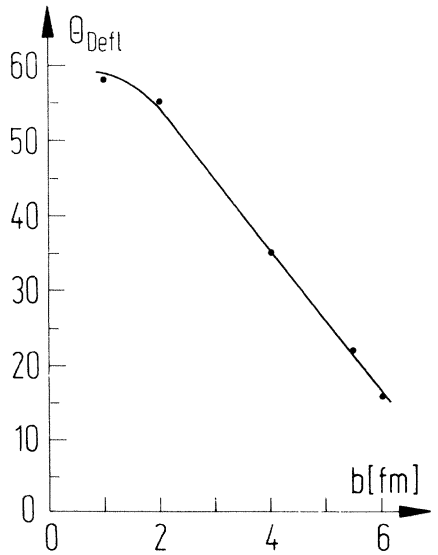

FIG. 7. Deflection angle of the projectile Θ_{defl} (obtained from the position of the maximum of the free nucleon cross section at $\phi = 0°$ and $E = 190$ MeV) versus the impact parameter b. There is a nearly linear impact parameter dependence for $b > 2$ fm.

TABLE II. Dependence of ρ_{max}, T_{max}, $\overline{E_{heat}}$, and the deflection angle on the impact parameter for the 393 MeV/nucleon reaction Ne+U. The transport coefficients chosen were $\eta_0 = 14.2$ MeV fm$^{-2}c^{-1}$, $\xi_0 = 0$, and $\kappa = 0.0$ c/fm.

b (fm)	ρ_{max} ($1/\rho_0$)	T_{max} (MeV)	$\overline{E_{heat}}$ (MeV/nucleon)	θ_{defl}
2	2.30	40.8	24.3	55°
4	2.26	43.5	21.9	35°
6	1.93	42.5	15.9	20.7°

the bounce-off process mainly three effects can be studied simultaneously: the kinematic variables, bombarding energy, and impact parameter; the transport processes with the influence of viscosity and heat conduction (and through them the kinetic properties of nuclear matter); and the equation of state (its softness and the ratio between the thermal and compressional energy), which we did not study here. However, only when azimuthally dependent cross sections are available[1] is there a possibility of distinguishing between these effects. The identification of the reaction plane and the projectile and target hemisphere seems to be experimentally feasible[1,8,9]; different impact parameters may be selected via the deflection angle. One may study the viscosity and heat conductivity of nuclear matter when energy spectra and angular distributions are analyzed. The momentum transfer and therefore the deflection angle decrease with increasing b. The collective and thermal velocity components can be approximately determined from the cross sections[1,7,9] and this way the temperature may be determined for different parts of the emitted particles. Also, the relative abundance of the heavier to the lighter fragments is affected by the temperature and therefore by viscosity and heat conductivity. An increase of T can be obtained by increasing the viscosity or by softening the equation of state. Because the thermal energy is not distributed equally over projectile and target the emission of heavier fragments is predominantly expected on the target side.

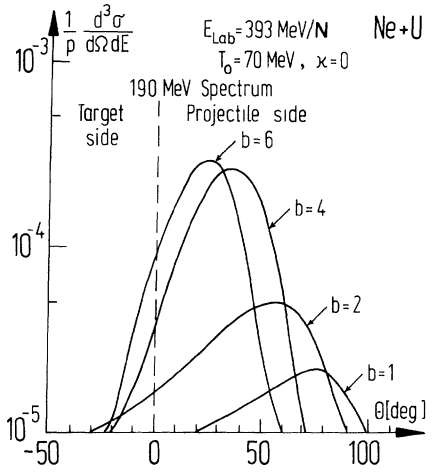

FIG. 8. 190 MeV cross sections for different impact parameters. With increasing b the deflection angle decreases and the importance of the bounce-off effect is enlarged (higher cross section).

Further information can be derived on the basis of three-dimensional calculations where apart from the target and projectile components of the cross section another component is predicted,[2] which is squeezed out orthogonally to the reaction plane and supplies direct information about the hot and dense (shocked) zone. Identification and more sophisticated experimental and theoretical analyses of these three components will lead to a deeper understanding of the reaction mechanism in high energy heavy ion collisions and the properties of hot and dense nuclear matter.

ACKNOWLEDGMENTS

This work was supported by the Bundesminister für Forschung und Technologie, by the Gesellschaft für Schwerionenforschung, Darmstadt, and by the Alexander von Humboldt Stiftung. One of us (L.P.C.) is an Alexander von Humboldt Research Fellow.

*On leave from the Central Research Institute for Physics, Budapest, Hungary.

[1] W. Meyer, H. H. Gutbrod, Ch. Lukner, and A. Sandoval, Phys. Rev. C 22, 179 (1980); H. H. Gutbrod, *Proceedings of the Symposium on Relativistic Heavy Ion Research, Darmstadt, 1978* (GSI, Darmstadt, 1978), p. 124.

[2] H. Stocker, J. Maruhn, and W. Greiner, Z. Phys. A 293, 173 (1979); Phys. Rev. Lett. 44, 725 (1980); H. Stocker, J. Hofmann, G. Buchwald, J. Maruhn, and W. Greiner, in *Proceedings of the European Physical Society Topical Conference on Large Amplitude Collective Nuclear Motions, Keszthely, Hungary, 1979* (Central Research Institute for Physics, Budapest, 1979), p. 761; Prog. Part. Nucl. Phys. 4, 133 (1980).

[3] G. D. Westfall *et al.*, Phys. Rev. Lett. 37, 1202 (1976).

[4] H. G. Baumgardt *et al.*, Z. Phys. A 273, 359 (1975).

[5] K. Wolf *et al.*, Phys. Rev. Lett. 42, 1448 (1979).

[6] A. Antonenko *et al.*, Zh. Eksp. Teor. Fiz. Pis'ma Red.

28, 609 (1978) [JETP Lett. 28, 561 (1978)]; *ibid.* 29, 103 (1979) [29, 94 (1979)].
[7]H. G. Baumgardt and E. Schopper, J. Phys. G 5, L231 (1979).
[8]A. Sandoval *et al.*, Phys. Rev. C 21, 1321 (1980).
[9]R. Stock *et al.*, Phys. Rev. Lett. 44, 1243 (1980).
[10]J. Otterlund, in *Proceedings of the Eighth International Conference on High Energy Physics and Nuclear Structure, Vancouver, 1979*, edited by D. F. Measday and A. W. Thomas (North-Holland, Amsterdam, 1980); and private communication.
[11]K. van Bibber *et al.*, Phys. Rev. Lett. 43, 840 (1979); D. K. Scott, Lectures at Alushta School on Nuclear Structure, Crimea, USSR, 1980 (unpublished).
[12]U. Lynen and H. Muller, private communication.
[13]W. Scheid, H. Muller, and W. Greiner, Phys. Rev. Lett. 32, 741 (1974); J. Hofmann *et al.*, *ibid.* 36, 88 (1976); J. Hofmann, W. Scheid, and W. Greiner, Nuovo Cimento 33A, 343 (1976).
[14]A. A. Amsden, G. F. Bertsch, F. H. Harlow, and J. R. Nix, Phys. Rev. Lett. 35, 905 (1975); A. A. Amsden, F. H. Harlow, and J. R. Nix, Phys. Rev. C 15, 2059 (1977); G. F. Bertsch and A. A. Amsden, *ibid.* 18, 1293 (1978).
[15]C. Y. Wong, J. Maruhn, and T. Welton, Nucl. Phys. A253, 469 (1975).
[16]H. Stöcker, J. Maruhn, and W. Greiner, Z. Phys. A 290, 297 (1979); H. Stöcker, R. Y. Casson, J. A. Moruhn, and W. Greiner, *ibid.* A 294, 125 (1980).
[17]L. P. Csernai, B. Lukács, and J. Zimányi, Lett. Nuovo Cimento 27, 111 (1980); in *Proceedings of the Seventh International Workshop on Gross Properties of Nuclei and Nuclear Excitations, Hirschegg, 1979*, edited by H. Feldmeier (Technische Hochschule, Darmstadt, 1979), p. 133.
[18]L. P. Csernai and H. W. Barz, Z. Phys. A 296, 173 (1980); L. P. Csernai, in *Proceedings of the Eighth International Workshop on Gross Properties of Nuclei and Nuclear Excitations, Hirschegg, 1980*, edited by H. Feldmeier (Technische Hochschule, Darmstadt, 1980), p. 36.
[19]H. H. Tang and C. Y. Wong, Phys. Rev. C 21, 1846 (1980).
[20]G. Buchwald, Ph.D. thesis, Universitat Frankfurt, 1980 (unpublished).
[21]P. Danielewicz, Nucl. Phys. A314, 465 (1979).
[22]L. P. Csernai, H. W. Barz, B. Lukács, and J. Zimányi, in *Proceedings of the European Physical Society Topical Conference on Large Amplitude Collective Nuclear Motions, Keszthely, 1979* (Central Research Institute for Physics, Budapest, 1979), p. 533; L. P. Csernai and B. Lukács, Central Research Institute for Physics, Budapest Report No. KFKI-79-58 (1979); L. P. Csernai and Gy. Fái, Central Research Institute for Physics, Budapest Report No. KFKI-79-66 (1979).
[23]A. Karvinen *et al.*, The Niels Bohr Institute, Copenhagen Report No. NBI-80-21 (1980).
[24]J. P. Bondorf, S. I. A. Garpmann, and J. Zimányi, Nucl. Phys. A296, 320 (1978); I. Montvay and J. Zimányi, *ibid.* A316, 490 (1979).
[25]L. D. Landau and E. M. Lifschitz, *Fluid Dynamics* (Pergamon, New York, 1953).
[26]K. Huang, *Statistical Mechanics* (Wiley, New York, 1963).
[27]R. Wieczorek, R. W. Hasse, and G. Süssmann, *Physics and Chemistry of Fission* (IAEA, Vienna, 1974, Vol. I, p. 523; J. R. Nix and A. P. Sierk, Los Alamos Scientific Laboratory Report No. LA-UR-79-1632 (1979).
[28]F. H. Harlow, A. A. Amsden, and J. R. Nix, J. Comp. Phys. 20, 119 (1976).
[29]E. Byckling and K. Kajantie, *Particle Kinematics* (Wiley, New York, 1973).
[30]M. Gyulassy, in *Proceedings of the European Physical Society Topical Conference on Large Amplitude Collective Nuclear Motions, Keszthely, 1979* (Central Research Institute for Physics, Budapest, 1979), p. 601.